RESEARCH

Slope stability analysis of a landfill subjected to leachate recirculation and aeration considering bio-hydro coupled processes

Shi-Jin Feng[1,2], Shao-Jie Wu[1], Wen-Ding Fu[1], Qi-Teng Zheng[1*] and Xiao-Lei Zhang[1,2]

Abstract

During the operation of landfills, leachate recirculation and aeration are widely applied to accelerate the waste stabilization process. However, these strategies may induce high pore pressures in waste, thereby affecting the stability of the landfill slope. Therefore, a three-dimensional numerical analysis for landfill slope stability during leachate recirculation and aeration is performed in this study using strength reduction method. The bio-hydro coupled processes of waste are simulated by a previously reported landfill coupled model programmed on the open-source platform OpenFOAM and then incorporated into the slope stability analysis. The results show that both increasing the injection pressure for leachate recirculation and maximum anaerobic biodegradation rate will reduce the factor of safety (*FS*) of the landfill slope maximally by 0.32 and 0.62, respectively, due to increased pore pressures. The ignorance of both waste biodegradation and gas flow will overestimate the slope stability of an anaerobic bioreactor landfill by about 20–50%, especially when the landfilled waste is easily degradable. The *FS* value of an aerobic bioreactor landfill slope will show a significant reduction (maximally by 53% in this study) when the aeration pressure exceeds a critical value and this value is termed as the safe aeration pressure. This study then proposes a relationship between the safe aeration pressure and the location of the air injection screen (i.e., the horizontal distance between the top of the injection screen and the slope surface) to avoid landfill slope failure during aeration. The findings of this study can provide insights for engineers to have a better understanding of the slope stability of a bioreactor landfill and to design and control the leachate recirculation and aeration systems in landfills.

Keywords: Landfill, Slope stability, Coupled processes, Leachate recirculation, Aeration

Introduction

Sanitary landfills still play a significant role in the disposal of Municipal Solid Waste (MSW) in most countries. Technologies including aeration and leachate recirculation have been applied to some landfills (Ritzkowski and Stegmann 2012; Stegmann 2019; Townsend et al. 2015) to accelerate the waste stabilization and reduce the methane emission potential. However, the addition of pressurized air and leachate would generate high pore pressures in

landfilled waste and reduce its effective stress and shear strength (Byun et al. 2019; Stoltz et al. 2012). An unreasonable design of aeration and recirculation systems might even cause catastrophes such as landfill slope failure and incidental environmental pollution and casualties (Feng et al. 2021a; Koerner and Soong 2000; Lavigne et al. 2014). Thus, it is important to evaluate the influence of leachate recirculation and aeration on the landfill slope stability and provide some guidelines that balance the efficiency of waste stabilization and the safety of landfill slope.

The distribution of pore pressures and the change in landfill slope stability during leachate recirculation have been studied by many researchers. For instance, Xu et al.

*Correspondence: 08qitengzheng@tongji.edu.cn
[1] Department of Geotechnical Engineering, Tongji University, Si Ping Road 1239, Shanghai 200092, China
Full list of author information is available at the end of the article

Feng *et al. Geoenvironmental Disasters*   (2021) 8:29

Page 2 of 16

(2012) and Feng et al. (2018) utilized the limit equilibrium method (LEM) and strength reduction method (SRM) to evaluate the stability of a landfill slope recirculated by horizontal wells and vertical wells, respectively. Feng et al. (2018) also developed a simple design method for vertical leachate injection wells considering both slope stability and recirculation efficiency. However, the waste biodegradation and landfill gas flow that would significantly affect the redistribution of pore pressures and the reduction of waste effective stress during recirculation (Lu et al. 2019) were generally neglected in most numerical analyses for landfill slope stability (Byun et al. 2019; Feng et al. 2018; Koerner and Soong 2000; Xu et al. 2012). Compared with soil, MSW is characterized by complicated biodegradation that is sensitive to the environment such as water saturation and oxygen concentration. Many environmental disasters induced by landfills are closely related to the biodegradation of MSW, and the generation and migration of gas and leachate in landfills (Lu et al. 2020). Therefore, the stability analysis of a bioreactor landfill slope should consider waste biodegradation and the corresponding multi-phase flow.

For landfill aeration, several numerical models under different conditions have been developed by previous researchers (Cao et al. 2018; Feng et al. 2019, 2021b; Fytanidis and Voudrias 2014; Lu and Feng 2020; Ma et al. 2020; Omar and Rohani 2017). For example, Fytanidis and Voudrias (2014) considered both the waste aerobic biodegradation and multi-phase flow in landfills under aeration based on the finite volume method (FVM). Cao et al. (2018) further considered the existence of both the aerobic reaction and anaerobic reaction of waste in a landfill. Lu and Feng (2020) presented a comprehensive overview of the mathematical formulations of biochemical, hydraulic, mechanical, and thermal processes in this coupled problem. These studies make a significant contribution to better understanding the coupled processes in aerobic landfills. However, to the best of the authors' knowledge, few studies have further focused on the impact of aeration on the landfill slope stability, which might be a concern for landfill engineers.

In this paper, a three-dimensional numerical analysis for landfill slope stability during leachate recirculation and aeration is performed using strength reduction method. Different from previous studies, the redistribution of pore pressures in waste is calculated by a previously reported two-phase flow model with fluid generation due to anaerobic/aerobic waste biodegradation. Hence, the responses of accelerated waste biodegradation and leachate-gas flow during recirculation and aeration can be incorporated into the slope stability analysis. Various recirculation and aeration scenarios are then simulated to provide some guidelines for the design of leachate/air injection systems considering the slope stability of landfills.

Methods

This section firstly introduces the bio-hydro coupled model for waste that was reported and validated by Lu et al. (2020). On this basis, the stability analysis method for landfill slope and the numerical implementation of the entire process are presented in this study to investigate the effects of leachate recirculation and aeration. The following assumptions were adopted in the numerical modelling: (1) landfill gas and leachate were immiscible, and their migrations can be described by Darcy's law; (2) leachate was incompressible, and landfill gas was assumed as ideal gas; (3) the intermediate products of waste biodegradation processes were neglected; (4) and the small-strain assumption was applied to calculate waste deformation.

Bio-hydro coupled model
Fluid flow equations
Gas and leachate flow in landfills can be described by the classic two-phase flow model for unsaturated porous materials as follows:

$$\frac{\partial(n\rho_\alpha S_\alpha)}{\partial t} + \nabla \cdot (\rho_\alpha \mathbf{v}_\alpha) = Q_\alpha \ \ (\alpha = \mathrm{g}, \mathrm{l}) \tag{1}$$

where n is the porosity of waste; S_α, ρ_α (kg/m^3) and $\mathbf{v}_\alpha$ (m/s) are the saturation degree, density, and Darcy velocity of phase α (g for gas and l for leachate), respectively, and $S_\mathrm{g} + S_\mathrm{l} = 1$; and Q_α (kg/m^3/s) is the source term of phase α due to biodegradation. The Darcy velocities of gas and leachate can be calculated according to Darcy's law as:

$$\mathbf{v}_\alpha = -\frac{\mathbf{K}_\alpha}{\mu_\alpha}\left(\nabla p_\alpha - \rho_\alpha \mathbf{g}\right) \tag{2}$$

where the tensor field $\mathbf{K}_\alpha$ (m^2) is the permeability of phase α in waste; μ_α (kg/m/s) and p_α (Pa) are the dynamic viscosity and pore pressures of phase α, respectively; and $\mathbf{g}$ (m/s^2) is the gravitational acceleration.

The leachate and gas permeability of landfilled waste can be expressed as:

$$\mathbf{K}_\alpha = \begin{pmatrix} AK_\mathrm{v} & & \\ & AK_\mathrm{v} & \\ & & K_\mathrm{v} \end{pmatrix} k_{\mathrm{r}\alpha} \tag{3}$$

where A is the anisotropic coefficient of waste; K_v (m^2) is the vertical intrinsic permeability of waste; and $k_{\mathrm{r}\alpha}$ is the relative permeability of phase α, which can be estimated by van Genuchten–Mualem model as follows (Mualem 1976; van Genuchten 1980):

Feng *et al. Geoenvironmental Disasters* (2021) 8:29

Page 3 of 16

$$\begin{cases} k_{rg} = (1 - S_{le})^{1/2} \left(1 - S_{le}^{1/m}\right)^{2m} \\ k_{rl} = S_{le}^{1/2} \left[1 - \left(1 - S_{le}^{1/m}\right)^m\right]^2 \\ S_{le} = (S_l - S_r)/(S_m - S_r) \end{cases} \qquad (4)$$

where S_{le}, S_m, and S_r are the effective, maximum and residual leachate saturations, respectively; and m is a dimensionless constant for the model. The relationship between S_{le} and pore pressures (p_l and p_g) can be expressed by van Genuchten model as (Lu et al. 2020; van Genuchten 1980):

$$p_c = \begin{Bmatrix} p_g - p_l & (p_g > p_l) \\ 0 & (p_g \le p_l) \end{Bmatrix} = p_{c0}\left(S_{le}^{-1/m} - 1\right)^{1-m} \qquad (5)$$

where p_c (Pa) and p_{c0} (Pa) are the capillary pressure and the entry capillary pressure of gas, respectively.

The density of leachate was assumed as constant, while the density of gas mainly depends on the gas pressure, and its time derivative of density can be written as:

$$\frac{1}{\rho_g} \frac{\partial \rho_g}{\partial t} = \frac{1}{p_g} \frac{\partial p_g}{\partial t} + \frac{1}{M_g} \frac{\partial M_g}{\partial t} - \frac{1}{T} \frac{\partial T}{\partial t} \qquad (6)$$

where M_g (g/mol) is the average molecular weight of gas mixture; and T (K) is the temperature. Substituting Eqs. (2) and (6) into Eq. (1) yields:

$$\frac{1}{\rho_l} \nabla \cdot \left[\rho_l \frac{\mathbf{K}_l}{\mu_l} \left(\rho_l \mathbf{g} - \nabla p_l\right)\right] + \frac{\partial (nS_l)}{\partial t} = \frac{Q_l}{\rho_l} \qquad (7)$$

$$\frac{nS_g}{p_g} \frac{\partial p_g}{\partial t} + \frac{1}{\rho_g} \nabla \cdot \left[\rho_g \frac{\mathbf{K}_g}{\mu_g} \left(\rho_g \mathbf{g} - \nabla p_g\right)\right]$$
$$- \frac{\partial (nS_l)}{\partial t} + \frac{nS_g}{M_g} \frac{\partial M_g}{\partial t} - \frac{nS_g}{T} \frac{\partial T}{\partial t} = \frac{Q_g}{\rho_g}. \qquad (8)$$

$$\text{Reaction mode} = \begin{cases} \text{Aerobic degradation} & \text{If } p_{Og} \ge 100 \, \text{Pa} \Rightarrow RM = 1 \\ \text{Anaerobic degradation} & \text{If } p_{Og} < 100 \, \text{Pa} \Rightarrow RM = 0 \end{cases} \qquad (14)$$

Oxygen transport equations

In aeration scenarios, the oxygen concentration can significantly affect the reaction modes and the degradation rate of waste (Kim et al. 2007; Omar and Rohani 2017), thereby affecting the distribution of pore pressures. To evaluate the oxygen distribution in landfills, its mass conservation in gas phase can be written as:

$$\frac{\partial \left(nS_g C_O\right)}{\partial t} + \nabla \cdot \left(C_O \mathbf{v}_g\right) - \nabla \cdot \left(nS_g \mathbf{J}_O\right) = Q_O \qquad (9)$$

where C_O (kg/m^3), $\mathbf{J}_O$ (kg/m^2/s), and Q_O (kg/m^3/s) are the concentration, diffusive flux and source term of oxygen in gas phase, respectively. $\mathbf{J}_O$ can be calculated using Fick's law:

$$\mathbf{J}_O = -\tau D_O \nabla C_O \qquad (10)$$

where D_O (m^2/s) is the diffusion coefficient of oxygen in gas; and τ is the tortuosity factor for gas diffusion considering the effect of porosity and saturation, and is defined as (Millington and Quirk 1961):

$$\tau = S_l^{7/3} n^{1/3} \qquad (11)$$

The time derivative of C_O can be written as:

$$\frac{1}{C_O} \frac{\partial C_O}{\partial t} = \frac{1}{\rho_g Y_O} \frac{\partial \left(\rho_g Y_O\right)}{\partial t}$$
$$= \frac{1}{Y_O} \frac{\partial Y_O}{\partial t} + \frac{1}{p_g} \frac{\partial p_g}{\partial t} + \frac{1}{M_g} \frac{\partial M_g}{\partial t} - \frac{1}{T} \frac{\partial T}{\partial t} \qquad (12)$$

where Y_O is the mass fraction of oxygen ($C_O = \rho_g Y_O$). Incorporating Eq. (12) into Eq. (9) yields:

$$nS_g \rho_g \frac{\partial Y_O}{\partial t} + \nabla \cdot \left(\rho_g Y_O \mathbf{v}_g\right) - \nabla \cdot \left(nS_g \rho_g \tau D_O \nabla Y_O\right)$$
$$+ \rho_g \left(\frac{nS_g}{p_g} \frac{\partial p_g}{\partial t} + \frac{nS_g}{M_g} \frac{\partial M_g}{\partial t} - \frac{nS_g}{T} \frac{\partial T}{\partial t} - \frac{\partial nS_l}{\partial t}\right) Y_O = Q_O \qquad (13)$$

Biodegradation equations

The reaction mode of waste in landfills depends on the local concentration of oxygen. Kim et al. (2007) suggested a threshold pressure of oxygen required for aerobic biodegradation:

where p_{Og} (Pa) is the oxygen partial pressure and *RM* is the parameter used to represent different reaction modes. To calculate the source term due to biodegradation mentioned in Eqs. (7), (8) and (13), a Monod-type biodegradation sub-model considering the effect of leachate saturation was adopted in this study (El-Fadel et al. 1996; Fytanidis and Voudrias 2014; Lu et al. 2020; Omar and Rohani 2017), which can be expressed as:

Feng *et al. Geoenvironmental Disasters*   (2021) 8:29

Page 4 of 16

$$R_A = \frac{\partial X_A}{\partial t} = k_{A,max} f_s \frac{S}{S_A + S} \frac{p_{Og}/p_g}{k_O + p_{Og}/p_g} X_A - R_{A,D} \tag{15}$$

$$R_N = \frac{\partial X_N}{\partial t} = k_{N,max} f_s \frac{S}{S_N + S} X_N - R_{N,D} \tag{16}$$

where R_A (kg/m^3/day) and R_N (kg/m^3/day) are the growth rates of aerobic and anaerobic species, respectively; X_A (kg/m^3) and X_N (kg/m^3) are the concentration of aerobic and anaerobic species, respectively; $k_{A,max}$ (day^{-1}) and $k_{N,max}$ (day^{-1}) are the maximum biodegradation rates under aerobic and anaerobic conditions, respectively; f_s is the leachate saturation correction factor; S (kg/m^3) is the biodegradable substrate concentration; S_A (kg/m^3) and S_N (kg/m^3) are the half-saturation constants of the substrates for aerobic and anaerobic species, respectively; k_O (kg/m^3) is the oxygen half-saturation constant; and $R_{A,D}$ (kg/m^3/day) and $R_{N,D}$ (kg/m^3/day) are the decay rates of aerobic and anaerobic species, respectively. $R_{A,D}$ and $R_{N,D}$ can be expressed as:
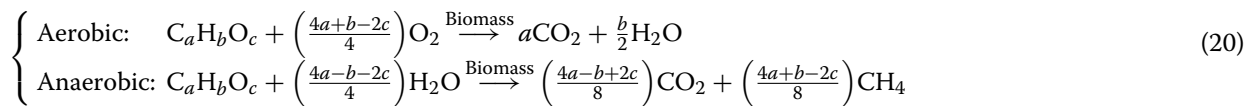
$$R_{A,D} = 0.05 k_{A,max}(X_A - X_{A,0}) \tag{17}$$

$$R_{N,D} = 0.05 k_{N,max}(X_N - X_{N,0}) \tag{18}$$

where $X_{N,0}$ (kg/m^3) and $X_{A,0}$ (kg/m^3) are the initial concentrations of anaerobic and aerobic species, respectively. The leachate saturation correction factor f_s can be expressed as (Meima et al. 2008):

$$f_s = \begin{cases} 0 & (S_l < 0.2) \\ \frac{S_l - 0.2}{0.3} & (0.2 \leq S_l \leq 0.5) \\ 1 & (0.5 < S_l) \end{cases} \tag{19}$$

The process of waste biodegradation can be described using the following chemical equations (Tchobanoglous et al. 1993):

$$R_M = \left[\left(\frac{4a + b - 2c}{8}\right)\frac{R_N}{Y_N} \times (1 - RM)\right]\frac{M_M}{M_{MSW}} \tag{21}$$

$$R_C = \left[\left(\frac{4a - b + 2c}{8}\right)\frac{R_N}{Y_N} \times (1 - RM) + a\frac{R_A}{Y_A} \times RM\right]\frac{M_C}{M_{MSW}} \tag{22}$$

$$R_O = \left[-\left(\frac{4a + b - 2c}{8}\right)\frac{R_A}{Y_A} \times RM\right]\frac{M_O}{M_{MSW}} \tag{23}$$

$$R_H = \left[-\left(\frac{4a - b - 2c}{4}\right)\frac{R_N}{Y_N} \times (1 - RM) + \frac{b}{2}\frac{R_A}{Y_A} \times RM\right]\frac{M_H}{M_{MSW}} \tag{24}$$

where Y_N and Y_A are the biomass/substrate yield coefficients of anaerobic and aerobic conditions respectively. Therefore, the aforementioned source terms Q_l, Q_g, and Q_O can be written as:

$$\begin{cases} Q_l = R_H \\ Q_g = R_C + R_M + R_O \\ Q_O = R_O \end{cases} \tag{25}$$

Slope stability analysis

The finite volume method (FVM) is usually used to deal with computational fluid dynamics problems. The introduced bio-hydro coupled model for waste has been programmed into the OpenFOAM platform based on FVM by Lu et al. (2020). This section is to add a sub-program for slope stability analysis based on the strength reduction method, which can expand the application of FVM in the deformation analysis of solid phase.

The pore pressures calculated by the bio-hydro coupled model will be directly imported into the slope

$$\begin{cases} \text{Aerobic:} & C_aH_bO_c + \left(\frac{4a+b-2c}{4}\right)O_2 \xrightarrow{\text{Biomass}} aCO_2 + \frac{b}{2}H_2O \\ \text{Anaerobic:} & C_aH_bO_c + \left(\frac{4a-b-2c}{4}\right)H_2O \xrightarrow{\text{Biomass}} \left(\frac{4a-b+2c}{8}\right)CO_2 + \left(\frac{4a+b-2c}{8}\right)CH_4 \end{cases} \tag{20}$$

where $C_aH_bO_c$ is the molecular formula of waste depending on its chemical composition; and a, b and c are the constants representing the contents of carbon, hydrogen and oxygen, respectively (Feng et al. 2021b). According to the law of mass conservation and Eq. (20), the production rates of methane R_M (kg/m^3/day) and carbon dioxide R_C (kg/m^3/day), and the consumption rates of oxygen R_O (kg/m^3/day) and water R_H (kg/m^3/day) can be calculated as follows:

stability analysis. The effective stress can be calculated based on the effective stress principle of unsaturated soil (Khoei and Mohammadnejad 2011):

$$d\boldsymbol{\sigma}' = d\boldsymbol{\sigma} + b\mathbf{I}dp \tag{26}$$

where $\boldsymbol{\sigma}'$ (Pa) and $\boldsymbol{\sigma}$ (Pa) denote the effective stress and total stress, respectively; b is the Biot coefficient; $\mathbf{I}$ is the identity tensor; and p (Pa) is the average pore pressure, which can be expressed as:

Feng *et al. Geoenvironmental Disasters*   (2021) 8:29

Page 5 of 16

$$p = p_l S_l + p_g S_g \tag{27}$$

This study adopts the Mohr–Coulomb model to calculate the mechanical plastic strain of waste, as has been applied in several studies (Feng et al. 2020; Lu et al. 2019, 2020):

$$\begin{cases} f = (\sigma_1' - \sigma_3') + (\sigma_1' + \sigma_3') \sin\varphi - 2c\cos\varphi \\ g = (\sigma_1' - \sigma_3') + (\sigma_1' + \sigma_3') \sin\psi \end{cases} \tag{28}$$

where f and g are the yield function and plastic potential function, respectively; σ_1' (Pa) and σ_3' (Pa) are the maximum and minimum principal stresses, respectively; and c (Pa), ϕ (°), and ψ (°) are the cohesion, friction angle and dilation angle of waste, respectively. The plastic strain increment can be expressed as:

$$d\boldsymbol{\varepsilon}^p = \Lambda \frac{\partial g}{\partial \boldsymbol{\sigma}'}, \ \Lambda = \begin{cases} 0, & f < 0 \\ \Lambda, & f = 0 \end{cases} \tag{29}$$

where Λ is the plastic factor that can be calculated using the local return mapping method proposed by Clausen et al. (2007).

Based on the small-strain theory, Lu et al. (2020) derived the relationship between the plastic strain increment and deformation increment of waste as:

$$\begin{aligned} \nabla \cdot & \left\{ \mu\nabla(d\mathbf{u}) + \mu\nabla(d\mathbf{u})^T + \lambda I tr[\nabla(d\mathbf{u})] \right\} \\ & - \nabla \cdot \left[2\mu d\boldsymbol{\varepsilon}^p + \lambda I tr(d\boldsymbol{\varepsilon}^p) \right] \\ & = \nabla \cdot (b\mathbf{I} dp) - d(\rho\mathbf{g}) \end{aligned} \tag{30}$$

where μ and λ are Lame constants which can be derived from Young's modulus E_s and Poisson's ratio v; and $\mathbf{u}$ (m) is the displacement vector.

This study adopts the strength reduction method (SRM) to analyze the stability of a landfill slope during recirculation and aeration. The SRM is suitable for linear Mohr–Coulomb failure criterion and has been widely used in the stability analysis of rock slopes (Yuan et al. 2020), soil slopes (Dawson et al. 1999; Griffiths and Lane 1999), and landfill slopes (Feng et al. 2018, 2020). The factor of safety is defined as the number by which the original shear strength parameters are divided to bring the slope to the point of failure, which is the same as that used in the traditional limit equilibrium method (Griffiths and Lane 1999). Therefore, the response of waste deformation can be examined by reducing the shear strength parameters in Eq. (28) following:

$$\begin{cases} c_r = \frac{c}{FS} \\ \varphi_r = \arctan\left(\frac{\tan\varphi}{FS}\right) \end{cases} \tag{31}$$

where FS is the factor of safety. By gradually increasing the value of FS, the slope will eventually reach an unstable state at which the displacement calculated by Eqs. (26)–(30) shows a dramatic increase. The FS at this moment reaches the real FS.

Numerical model implementation

Equations (7), (8), (13), and (30) are the main governing equations for the landfill coupled model established in this study. There are four independent unknown variables: leachate pressure p_l, gas pressure p_g, mass fraction of oxygen in gas phase Y_O, and displacement increment $d\mathbf{u}$. Other variables can be derived based on the above basic variables.

Based on FVM, the governing equations of the coupled model are discretized with the Gauss divergence theorem which converts the volume integrals of the governing equations over a specific volume into surface integrals. The detailed information on the discretization process can be found in Lu et al. (2020) and Weller and Tabor (1998). Finally, the implicit term is converted into a matrix of unknown variables; and the explicit terms such as source terms can be calculated using the results obtained in the previous iteration or time step.

After discretizing, the governing equations in the centroid C of each control volume can be transformed and rearranged into linear algebraic equations as follows:

$$\begin{cases} \beta_C^{p_\alpha}(p_\alpha)_C + \sum_N \beta_N^{p_\alpha}(p_\alpha)_N = R_C^{p_\alpha} \\ \beta_C^{Y_O}(Y_O)_C + \sum_N \beta_N^{Y_O}(Y_O)_N = R_C^{Y_O} \\ \beta_C^{d\mathbf{u}}(d\mathbf{u})_C + \sum_N \beta_N^{d\mathbf{u}}(d\mathbf{u})_N = R_C^{d\mathbf{u}} \end{cases} \tag{32}$$

where β_C, β_N, and R_C are the diagonal coefficients, neighbor coefficients, and source terms, respectively. Assembling Eq. (32) for all control volumes as a whole, a system of linear equations can be obtained as:

$$\mathbf{B}F = \boldsymbol{b} \tag{33}$$

where $\mathbf{B}$ is a symmetric matrix; F is the unknown vector for leachate pressure, gas pressure, mass fraction of oxygen, and displacement increment; and $\boldsymbol{b}$ is the right-hand side vector.

Figure 1 shows the overall procedures of the solver based on the sequential iteration method. At each iteration of time step t, the fluid flow equations, the oxygen transport equation, and the displacement equation are solved in sequence, with the related parameters and source terms being updated. The convergence criteria of the calculation are defined as:

$$\begin{cases} \max \left| F^{t+1,n+1} - F^{t+1,n} \right| \leq \varepsilon_F \\ \max \left| \frac{F^{t+1,n+1} - F^{t+1,n}}{F^{t+1,n+1}} \right| \leq \zeta_F \end{cases} \tag{34}$$
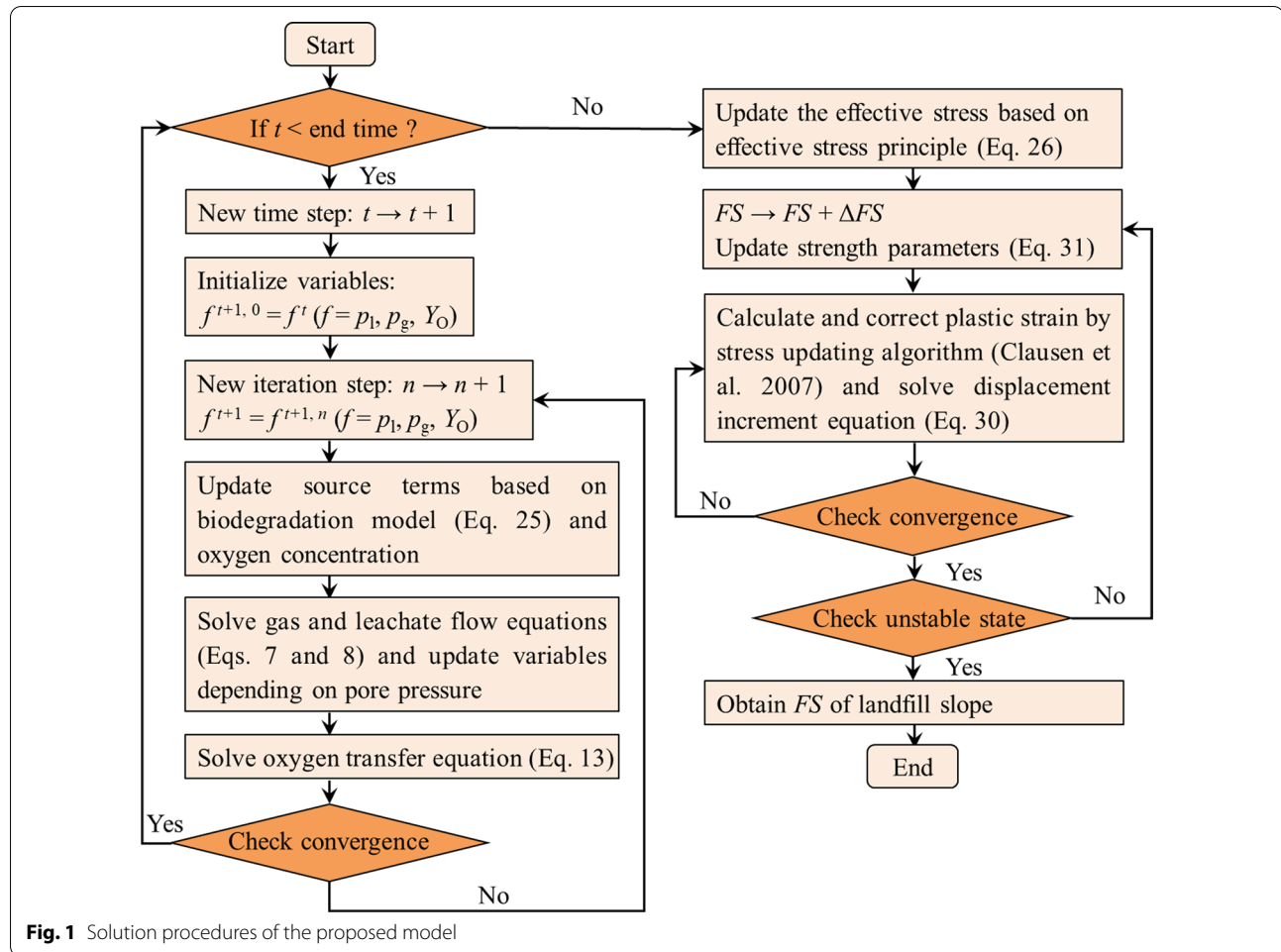
Feng *et al. Geoenvironmental Disasters* (2021) 8:29

Page 6 of 16

Fig. 1 Solution procedures of the proposed model

where ε_F and ζ_F are the absolute and relative convergence tolerances for variable F, respectively. The local return mapping method is adopted to obtain the modified plastic strain increment using the pore pressure calculated in the previous section. The detailed information about the algorithm can be found in Clausen et al. (2007) and Tang et al. (2015). The strength parameters c and ϕ are gradually reduced to examine the response of deformation until a dramatic increase in the displacement. Based on FVM, the code for the waste bio-hydro coupled model and landfill slope stability analysis are implemented in the C++ based open-source platform OpenFoam. The code is flexible in dimensionality and can solve problems in one dimension, two dimensions, and three dimensions (Lu et al. 2019, 2020).

Results and discussion
Conceptual model and parameter selection
A three-dimensional conceptual model of a landfill slope is established with a cover on the top and a leachate collection and removal system at the bottom (Fig. 2a). In leachate recirculation scenarios (Fig. 2b), a horizontal trench (1 m × 1 m) for leachate addition with a continual pressure of P_{li} (kPa) is installed 30 m above the bottom of a 50-m high and 180-m wide landfill with a slope gradient of $1{:}\lambda = 1{:}3$. The slope geometry of leachate recirculation scenarios is the same as those in Xu et al. (2012) and Feng et al. (2018) for comparison of *FS* in the next section. In aeration scenarios (Fig. 2c), the landfill slope has a height of 25 m, a width of 80 m and a slope gradient of $1{:}\lambda = 1{:}3$. A smaller landfill height is adopted because the influence radius of aeration wells is generally less than 10 m (Fytanidis and Voudrias 2014), and hence the effect of aeration on the slope stability can be presented more clearly. A vertical air injection screen with a length of 3 m, a diameter of 0.3 m, and an injection pressure of P_{gi} (kPa) is placed 15 m vertically above the bottom of the landfill. The horizontal distance between the top of air injection screen and the slope surface is defined as d. The d ranges between 5 and 10 m in the following to investigate its effect on *FS*.
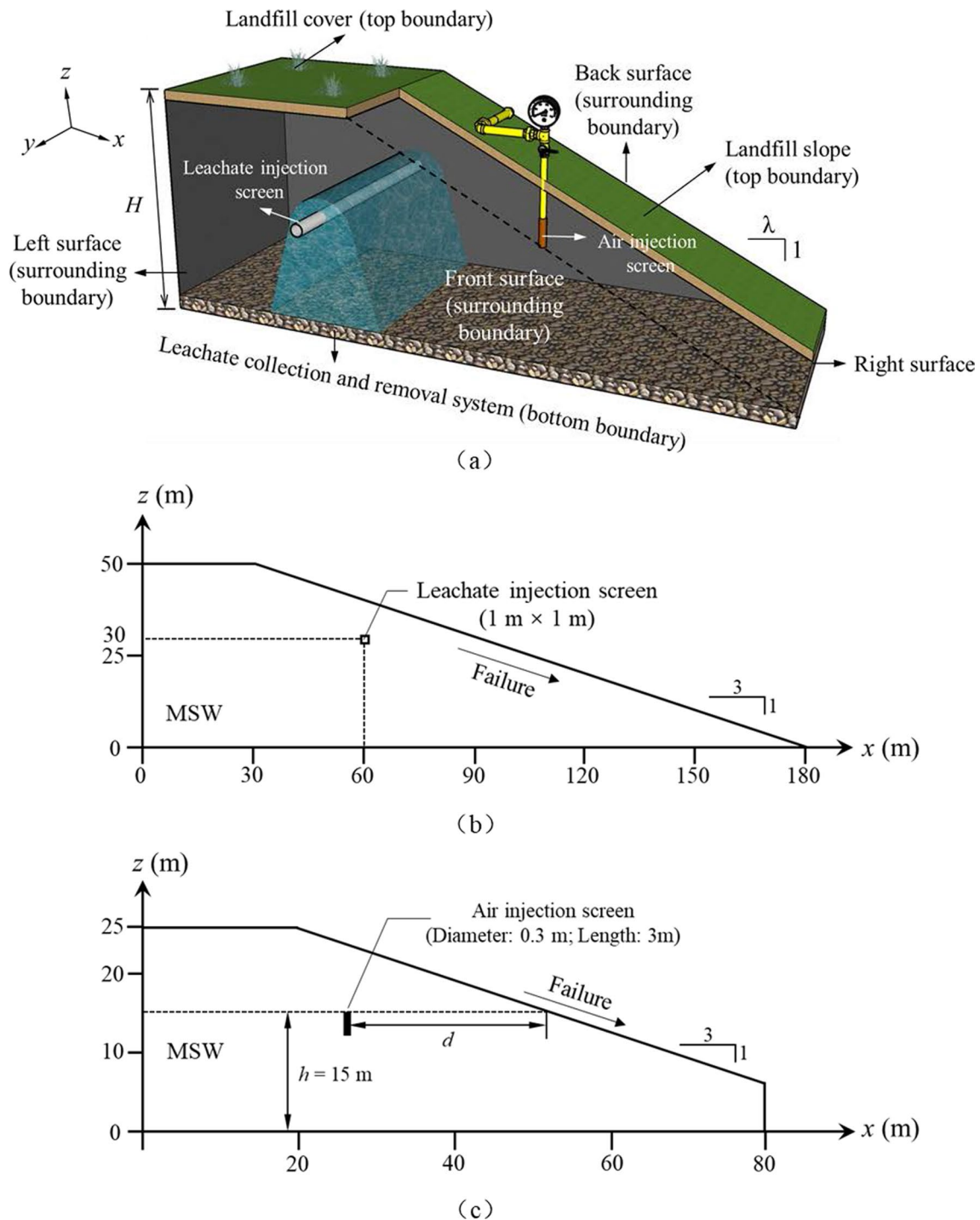
Fig. 2 Schematic of a bioreactor landfill with slope: **a** 3D view of the conceptual model; **b** cross-sectional view of leachate injection scenario; **c** cross-sectional view of air injection scenario

Boundary conditions for numerical modelling are presented in Table 1. The surrounding boundaries (the left, back, and front boundaries in Fig. 1a) were set as symmetrical. The top boundary can move freely during waste deformation and was regarded as impermeable to leachate without consideration of rainfall infiltration and evaporation. An atmospheric pressure was also set at the top. At the bottom surface, the leachate pressure

Feng *et al. Geoenvironmental Disasters*   (2021) 8:29

Page 8 of 16

was fixed at zero for free drainage and the displacement was constrained in every direction. Both the bottom surface and the leachate injection trenches were assumed as impermeable to gas since the surrounding waste is generally saturated by leachate. Similarly, the air injection screens were assumed as impermeable to leachate and the mass fraction of oxygen was fixed at 26.6% as in the atmosphere. The right surface was assumed as impermeable to both leachate and gas due to the existence of an engineered berm at the toe of landfill slope. The initial stress and displacement fields are obtained by solving Eqs. (28)–(30) under gravity.

Default model parameters for slope stability analysis are listed in Tables 2, 3 and 4. The biokinetic parameter values for waste listed in Table 2 are selected based on the previous experiments on waste biodegradation

Table 1 Boundary conditions for numerical simulations

Boundaries	Top surface	Bottom surface	Right surface	Surrounding surfaces	Leachate injection trench	Air injection screen
p_g	Fixed value (0 Pa)	Impervious	Impervious	Symmetry	Impervious	Fixed value (1–15 kPa)
p_l	Impervious	Fixed value (0 Pa)	Impervious	Symmetry	Fixed value (49–343 kPa)	Impervious
Y_O	Fixed value (0%)	Zero gradient	Zero gradient	Symmetry	Fixed value (0%)	Fixed value (26.6%)
du	Free traction	Fixed	$du_x = 0$	Symmetry	–	–

Table 2 Biokinetic parameters used in this paper

Parameter	Unit	Value	References
Maximum anaerobic biodegradation rate $k_{A,max}$	day^{-1}	1	Kim et al. (2007)
Maximum aerobic biodegradation rate $k_{N,max}$	day^{-1}	0.02	Kim et al. (2007)
Oxygen half-saturation constant for aerobic growth k_O	–	0.07	Kim et al. (2007)
Substrate half-saturation constant for aerobic growth $S_{A,S}$	kg/m^3	100	Estimated from model
Substrate half-saturation constant for anaerobic growth $S_{N,S}$	kg/m^3	50	Estimated from model
Initial concentration of aerobic biomass $X_{A,0}$	kg/m^3	0.15	Omar and Rohani (2017)
Initial concentration of anaerobic biomass $X_{N,0}$	kg/m^3	0.15	Omar and Rohani (2017)
Aerobic biomass yield coefficient Y_A	kg B/kg S	0.1	Beaven et al. (2008)
Anaerobic biomass yield coefficient Y_N	kg B/kg S	0.05	Kim et al. (2007)
Molecular weights of oxygen M_{MSW}	g/mol	162	Fytanidis and Voudrias (2014)

Table 3 Hydraulic parameters used in this paper

Parameter	Unit	Value	References
Waste density ρ_s	kg/m^3	1500	Feng et al. (2018), Feng et al. (2020), Xu et al. (2012)
Initial gas density ρ_g	kg/m^3	1.25	
Leachate density ρ_l	kg/m^3	1000	
Porosity n	–	0.5	
Initial leachate saturation S_{l0}	–	0.5	
Initial gas pressure p_{g0}	Pa	0	
Vertical intrinsic permeability K_v	m^2	10^{-12}	
Diffusion coefficient of oxygen D_O	m^2/s	2×10^{-5}	Feng et al. (2021b), Lu et al. (2020)
Dynamic viscosity of gas μ_g	kg/m/s	1.37×10^{-5}	
Dynamic viscosity of leachate μ_l	kg/m/s	10^{-3}	
Van Genuchten parameter p_{c0}	Pa	4900	Fytanidis and Voudrias (2014), Lu et al. (2020)
Van Genuchten parameter m	–	0.5	
Residual saturation $S_{w,r}$	–	0.2	
Maximum saturation $S_{w,m}$	–	0.99	

Feng *et al. Geoenvironmental Disasters* (2021) 8:29

Page 9 of 16

Table 4 Mechanical parameters used in this paper

Parameter	Unit	Value	References
Young's modulus E_s	kPa	225	Lu et al. (2020)
Poisson's ratio v	–	0.4	
Biot coefficient b	–	1	
Dilation angle for waste ψ	degree	0	
Friction angle for waste φ	degree	35	Xu et al. (2012)
Waste cohesion c	kPa	15	

(Beaven et al. 2008; Fytanidis and Voudrias 2014; Kim et al. 2007; Omar and Rohani 2017) and have also been adopted by Cao et al. (2018) and Feng et al. (2021b). The organic matter of waste is represented by $C_6H_{10}O_5$ in this study. Tables 3 and 4 list the detailed hydraulic and mechanical parameters, respectively. Typical values of van Genuchten parameters p_{c0} (4900 Pa) and m (0.5), residual saturation $S_{w,r}$ (0.2), and maximum saturation $S_{w,m}$ (0.99) are adopted (Fytanidis and Voudrias 2014). The waste properties (i.e., density, porosity, permeability, strength parameters, and initial conditions) adopted in this work are similar to those in Xu et al. (2012) and Feng et al. (2018) for comparison.

Model validation
Lu et al. (2020) has validated the bio-hydro coupled model using experimental data. The stability analysis of landfill slope is verified with those reported in Xu et al. (2012) and Feng et al. (2018) where the leachate was recirculated by horizontal trenches. Xu et al. (2012) used GeoStudio, a finite element method (FEM) based

Fig. 3 Comparison of the relationships between *FS* and friction angle obtained by Feng et al. (2018), Xu et al. (2012) and the proposed model

program, while Feng et al. (2018) used FLAC, a finite difference method (FDM) based software. Thus, Fig. 3 presents the *FS* values for different friction angles calculated in the above two studies and by the proposed model without activating the gas flow and biodegradation sub-models. The small differences among the three curves are due to the differences in the calculation method (LEM in Xu et al. (2012) and SRM in Feng et al. (2018) and this paper) and the modeling approach (FEM in Xu et al. (2012), FDM in Feng et al. (2018) and FVM in this paper). However, the differences are acceptable for engineering practice and the *FS* values calculated in this paper are generally conservative. Subsequently, the proposed model can then be applied in the following.

Leachate recirculation scenarios
The conceptual landfill in Fig. 2b is simulated in this part to investigate the effects of waste biodegradation and gas flow on the slope stability under leachate recirculation. Four scenarios are presented in Table 5, which can be achieved by activating the corresponding sub-model of the proposed model. To describe waste non-homogeneity with depth, the porosity, density and vertical intrinsic permeability of waste were assumed to linearly decrease from 0.5, 1500 kg/m³ and 10^{-12} m² at $z = 50$ m (top) to 0.3, 1800 kg/m³ and 10^{-14} m² at $z = 0$ m (bottom), respectively. A typical anisotropic coefficient of 5 was selected to consider waste anisotropy. Simulations with 11,400 finite-volume meshes were conducted on a workstation with 16 cores.

Gas pressure in landfill
Initially, the effect of waste biodegradation on the distribution of gas pressure under recirculation using horizontal trenches is investigated ($P_{li} = 49$ kPa). Figure 4 compares the distributions of gas pressures at $x = 60$ m on the 5th, 10th, 20th, and 50th day in Scenarios 3 and 4. Overall, the gas pressures in both cases gradually increase over time due to the increased leachate saturation around the horizontal trench, and the gas pressures at the bottom of landfill are relatively higher since the leachate collection system is impermeable to gas. However, since the accelerated anaerobic degradation of waste will generate
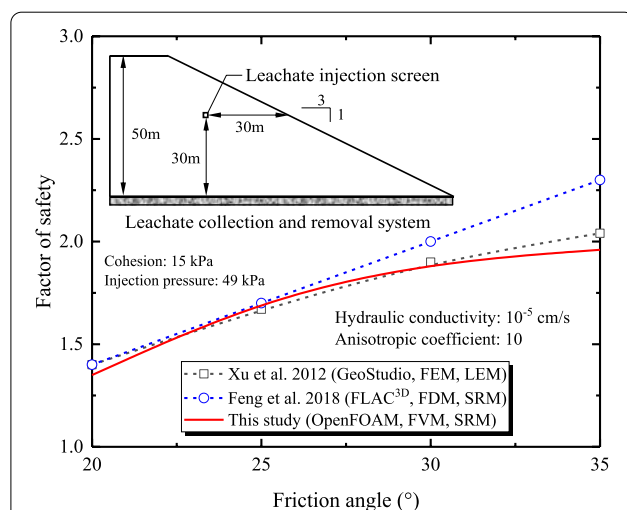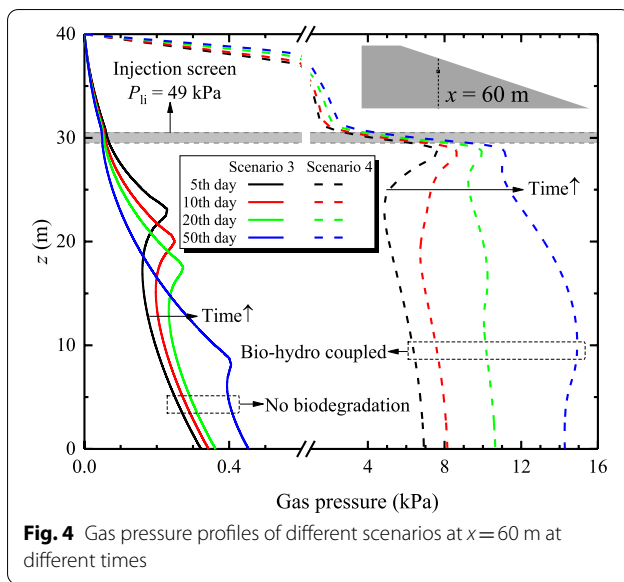
Table 5 Summary of leachate recirculation scenarios for comparison
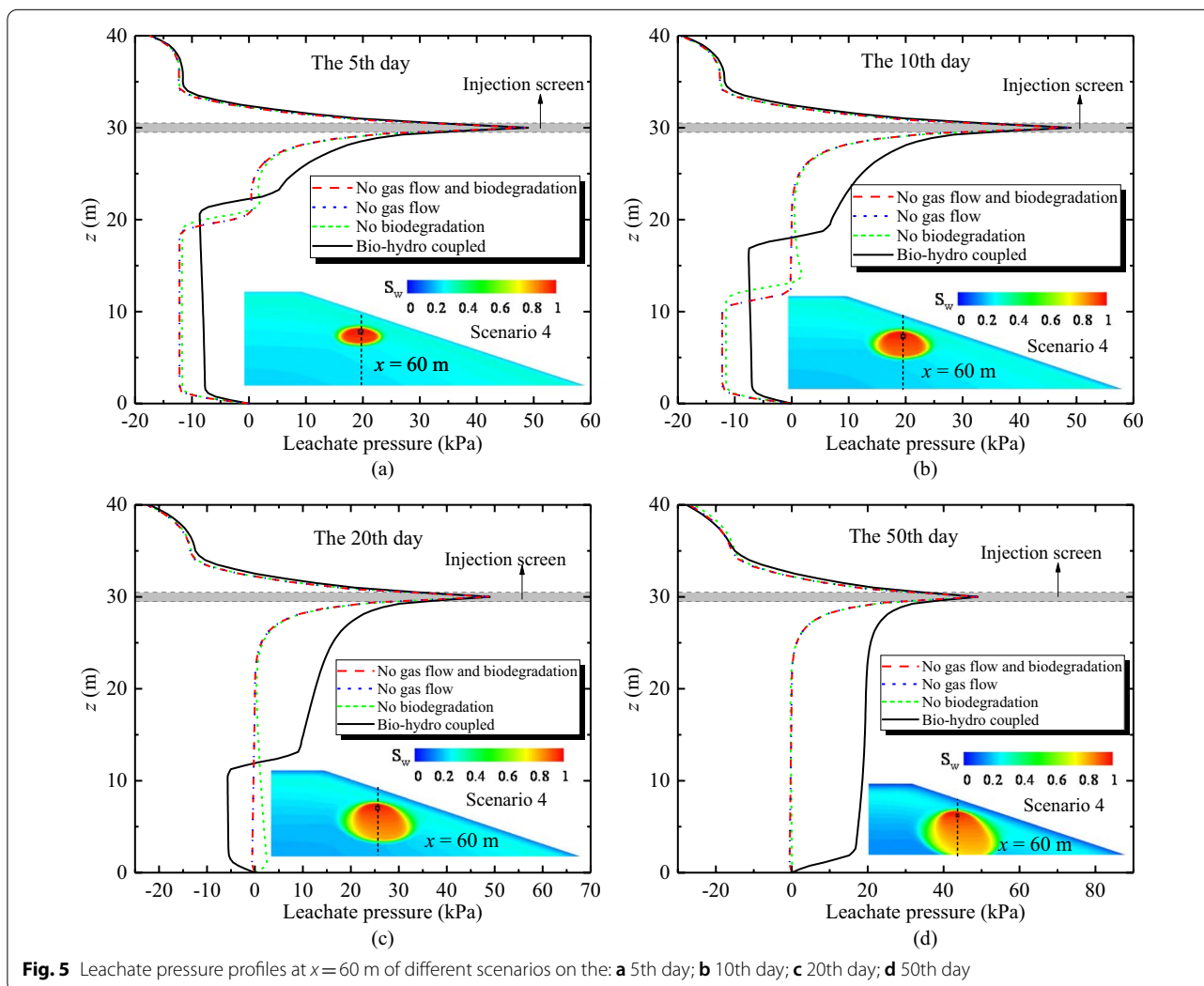
Scenario	Coupled type
Scenario 1	Neglecting gas flow and waste biodegradation
Scenario 2	Neglecting gas flow
Scenario 3	Neglecting waste biodegradation
Scenario 4	The proposed model in this study

Feng *et al. Geoenvironmental Disasters* (2021) 8:29

Page 10 of 16

Fig. 4 Gas pressure profiles of different scenarios at $x = 60$ m at different times

more gas, the gas pressure of Scenario 4 (0~16 kPa) is much larger than that of Scenario 3 (0~500 Pa) where waste biodegradation is neglected. Moreover, the gas pressure profiles of these two scenarios are totally different. In Scenario 3 without biodegradation, an evident turning point with a relatively high gas pressure can be observed at the front of infiltrated leachate. However, in Scenario 4, the turning point locates at the depth where the injected trench is installed because the higher leachate saturation around it can accelerate the gas generation and reduce the channel for gas migration at the same time (see Fig. 5).

Leachate pressure in landfill

Figure 5 depicts the leachate pressure profiles (relative to atmospheric pressure) at $x = 60$ m on the 5th, 10th, 20th, and 50th day in Scenarios 1–4 and the saturation contour of scenario 4 is also included for comparison. The leachate pressure profiles of Scenario 1 (no gas

Fig. 5 Leachate pressure profiles at $x = 60$ m of different scenarios on the: **a** 5th day; **b** 10th day; **c** 20th day; **d** 50th day

Feng *et al. Geoenvironmental Disasters* (2021) 8:29

Page 11 of 16

flow and biodegradation) and Scenario 2 (no gas flow) are almost the same, indicating that the effect of generated leachate can be neglected when ignoring the gas flow. The difference between Scenario 1 and Scenario 3 (no biodegradation) is also small because no gas is generated when ignoring biodegradation. However, a significantly different leachate pressure profile can be observed in Scenario 4 (bio-hydro coupled) and the difference becomes more and more obvious over time. This demonstrates that the combination of waste biodegradation and gas flow obviously affects the redistribution of leachate during recirculation. In all the four scenarios, negative leachate pressures can be found at the areas near the top and bottom of the landfill, referring to an unsaturated zone due to leachate drainage. When the landfilled waste is saturated by the injected leachate, the leachate pressure becomes positive. On the 20th day, the injected leachate from the buried horizontal trench can reach the bottom of the landfill in Scenarios 1–3, while in Scenario 4 there is still an unsaturated zone near the bottom since the generated gas impedes the leachate migration.
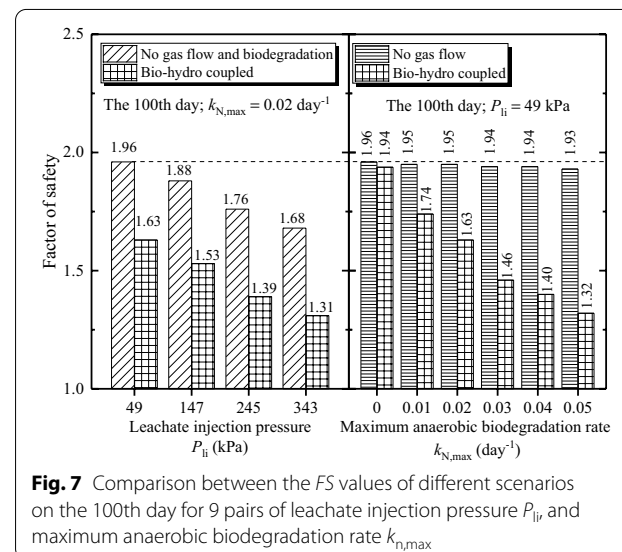
Many previous studies have neglected the effect of gas flow on leachate flow in an anaerobic bioreactor landfill. The results of this work manifest that this assumption is only reasonable in some cases where the organic content of landfilled waste is low and hence the waste biodegradation can be ignored. As a whole, both waste biodegradation and gas flow should be considered when analyzing the landfill gas and leachate flows, otherwise, the influence area and the performance of leachate recirculation would be overestimated.
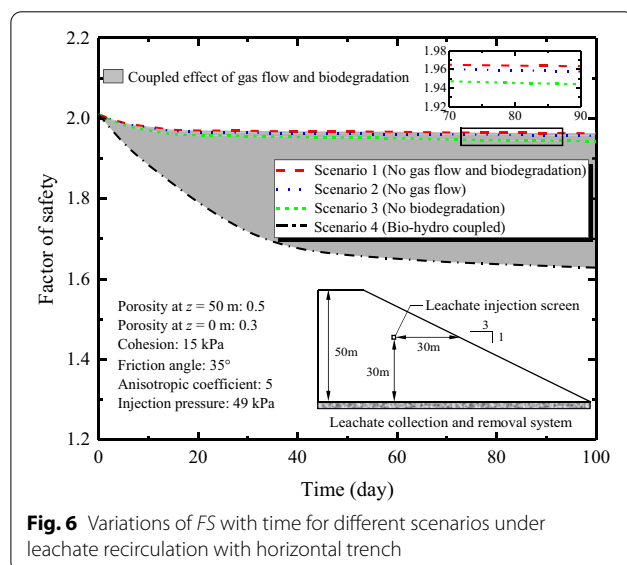
Factor of safety of landfill slope

Before recirculation, the *FS* value of the modeled landfill slope is about 2.01, but with an injection pressure of 49 kPa, the *FS* value shows a reduction over recirculation time (Fig. 6), which is consistent with the increased pore pressures mentioned above. A small difference in the *FS* values of Scenarios 1–3 can be observed, corresponding to similar pore pressures presented in Fig. 5. Scenario 4 (bio-hydro coupled) has the smallest value of *FS*, and the *FS* difference between Scenarios 1 (no gas flow and biodegradation) and 4 gradually increases over time until reaching 0.35 on the 100th day (shadow region in Fig. 6). This difference is attributed to an increasing difference in the pore pressures (see Figs. 4 and 5) when considering the waste biodegradation and gas flow during leachate recirculation.

To further investigate the bio-hydro coupled effect on the landfill slope stability, Fig. 7 presents the *FS* value on the 100th day for 9 pairs of leachate injection pressure ($P_{li} = 49$, 147, 245, and 343 kPa) and maximum anaerobic biodegradation rate ($k_{n,max} = 0$, 0.01, 0.02, 0.03, 0.04, and 0.05 day^{-1}). For the scenario with $k_{n,max} = 0$ day^{-1}, the waste biodegradation is neglected. All the *FS* values calculated by the proposed model range between 1.31 and 1.96 in Fig. 7, within the normal range reported in the previous similar studies (Byun et al. 2019; Feng et al. 2018, 2020; Xu et al. 2012). Both increasing the leachate injection pressure and maximum anaerobic biodegradation rate can reduce the *FS* value of a landfill slope maximally by 0.32 (at $P_{li} = 343$ kPa) and 0.62 (at $k_{n,max} = 0.05$ day^{-1}), respectively, due to the increased pore leachate and gas pressures. Moreover, the *FS* difference between the bio-hydro coupled model and the

Fig. 6 Variations of *FS* with time for different scenarios under leachate recirculation with horizontal trench

Fig. 7 Comparison between the *FS* values of different scenarios on the 100th day for 9 pairs of leachate injection pressure P_{li}, and maximum anaerobic biodegradation rate $k_{n,max}$

model ignoring gas flow and biodegradation ranges between 0.33 and 0.37 (left sub-figure in Fig. 7). If only ignoring the gas flow, the waste biodegradation and the produced leachate have a very slight effect on the landfill slope stability, i.e., from 1.96 to 1.93 in the right sub-figure of Fig. 7. However, the ignorance of both waste biodegradation and gas flow will largely overestimate the stability of a landfill slope by about 20–50% (e.g., (1.96–1.32)/1.32 = 46% for $k_{N, max} = 0.05$ day^{-1} and $P_{li} = 49$ kPa), especially when the landfilled waste has a high degradation rate and can then significantly increase the pore pressures.

Aeration scenarios

As one of the main strategies to accelerate waste biodegradation, aeration will increase the pore pressures of waste and then pose a threat to the landfill slope stability. In this part, the conceptual landfill in Fig. 2c is simulated using the proposed bio-hydro coupled model.

The porosity, density and vertical intrinsic permeability of waste were assumed to linearly decrease from 0.5, 1500 kg/m^3 and 10^{-12} m^2 at $z = 25$ m (top) to 0.4, 1700 kg/m^3 and 10^{-13} m^2 at $z = 0$ m (bottom), respectively. A waste anisotropy coefficient of 5 was adopted. The aeration pressure P_{gi} between 1 and 15 kPa was assumed base on engineering practice (Fytanidis and Voudrias 2014; Ritzkowski and Stegmann 2012; Townsend et al. 2015). A leachate saturation of 0.5, an atmospheric gas pressure, and an oxygen fraction of 0% were assumed as the initial condition. Simulations with 80,000 finite-volume meshes were conducted on a workstation with 16 cores.

Figure 8 shows the spatial distribution of gas pressure within the landfill in 3D view and cross-sectional view at $y = 10$ m on the 20th day of aeration with an injection pressure of 12 kPa. It can be observed that the gas pressure near the injection screen (about 9 ~ 12 kPa in red) and the bottom of the landfill (about 7 kPa in green) is significantly higher than that in other regions. The local accumulation of gas pressure within 3 m around the
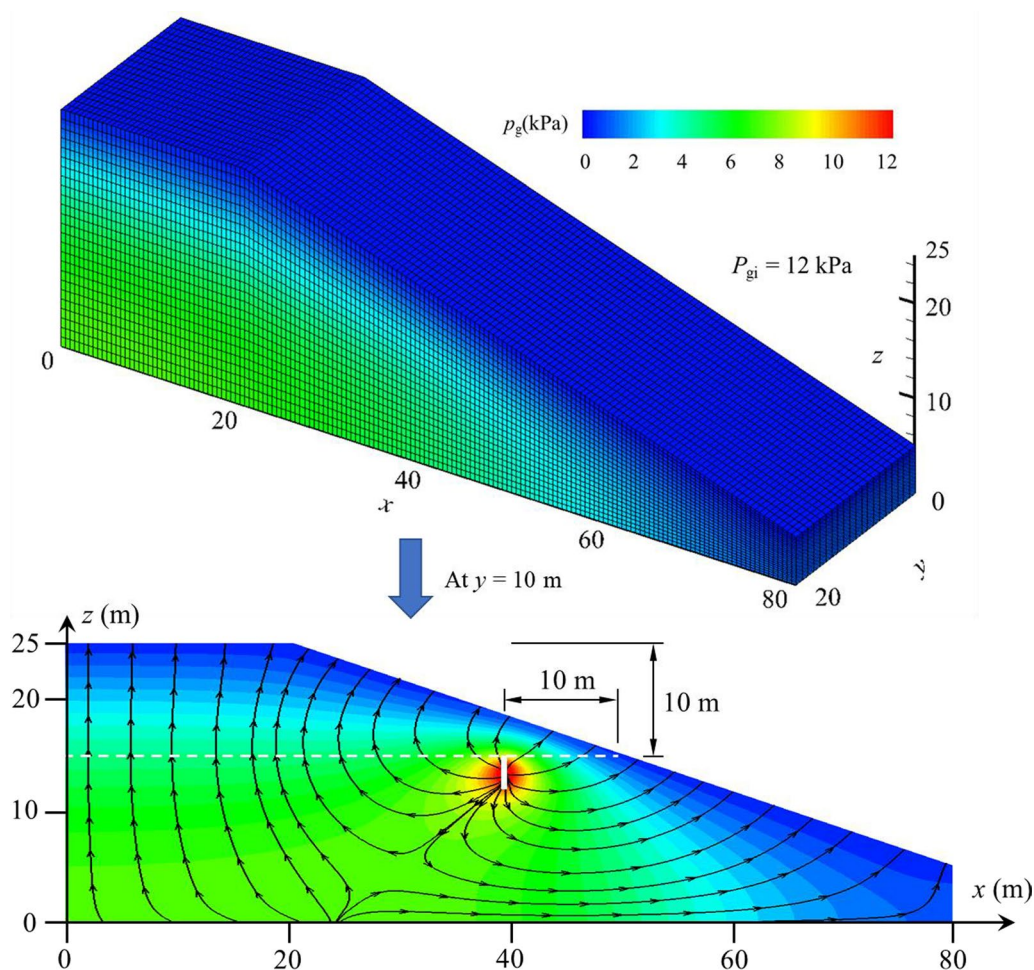

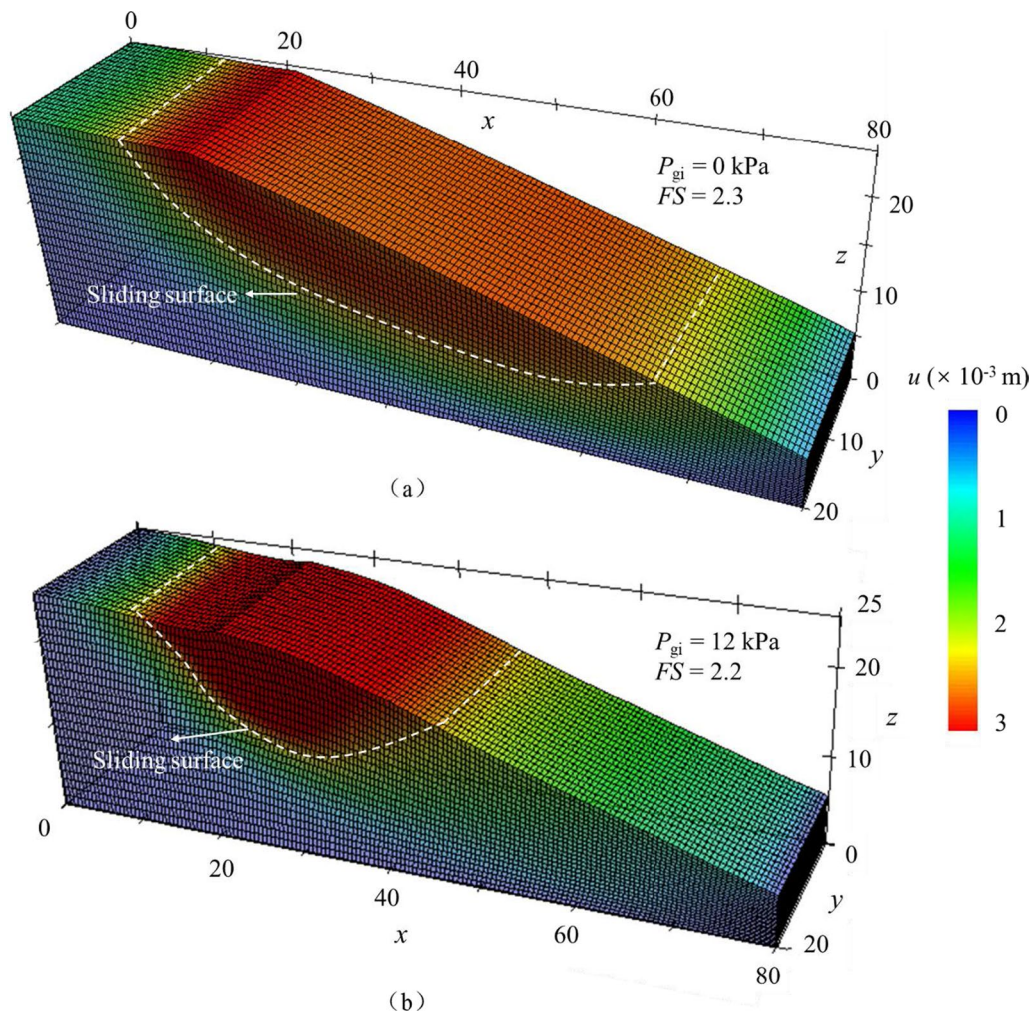**Fig. 8** The spatial distribution of gas pressure on the 20th day of aeration

Fig. 9 Possible slope failure mode in terms of the displacement at an unstable state: **a** $P_{gi}=0$ kPa; **b** $P_{gi}=12$ kPa

aeration well may be detrimental to the local stability of the landfilled waste. It should be noted that the gas pressure at the top was set as zero in this paper (in blue in Fig. 8) to represent an efficient gas collection system.

Figure 9 shows the effect of aeration on the stability of a landfill slope in terms of the displacement at an unstable state. Compared to the scenario without air injection, an injection pressure of 12 kPa will slightly reduce the value of *FS* by 0.1 (4.5%) when the horizontal distance between the top of the injection screen and the slope surface (*d*) is 10 m. However, these two scenarios have different slope failure modes. For $P_{gi}=0$, the overall slope is unstable and the possible sliding surface develops from the left platform to the toe of the landfill slope. When P_{gi} increases to 12 kPa, a local slope failure will occur before an overall instability mainly due to the accumulated gas pressures around the injection screen.

To further investigate the effect of aeration on the stability of a landfill slope, the changes of *FS* with air injection pressure P_{gi} for different values of *d* (i.e., the horizontal distance between the top of the injection screen and the slope surface) are obtained and plotted in Fig. 10. As might be expected, the value of *FS* gradually decreases with increasing aeration pressure from 2.3 at $P_{gi}=0$ kPa (without aeration). The reduction in *FS* is slight at low aeration pressure, but becomes significant and then poses a threat to the slope stability when the aeration pressure exceeds a critical value, defined as the safe aeration pressure P_{gs} below. The maximum reduction can reach up to 0.8 (about 53%, *FS*=1.5) for $P_{gi}=15$ kPa and *d*=5 m. Taking *d*=7 m as an example, the *FS* remains stable around 2.3 and begins to show a significant decrease when P_{gi} exceeds 3.8 kPa (red dash arrow in Fig. 10). Thus, $P_{gs}=3.8$ kPa when *d*=7 m, that
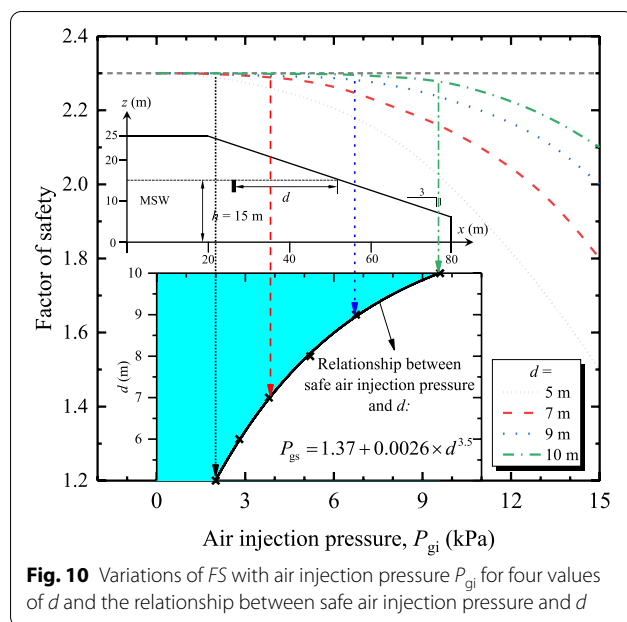
Feng *et al. Geoenvironmental Disasters* (2021) 8:29

Page 14 of 16

Fig. 10 Variations of *FS* with air injection pressure P_{gi} for four values of *d* and the relationship between safe air injection pressure and *d*

is, an aeration pressure of $P_{gi} \leq 3.8$ kPa is recommended for $d = 7$ m during the operation of aeration in practice to benefit the landfill slope stability. By identifying the safe aeration pressure P_{gs} for $d = 5 \sim 10$ m, a unique relationship between P_{gs} and *d* can be observed in Fig. 10 (black solid line). P_{gs} increases from 2 kPa at $d = 5$ m to 9.6 kPa at $d = 10$ m. These recommended aeration pressures regarding to the safety of the landfill slope are consistent with the values that are widely adopted in many aerobic projects, i.e., $2 \sim 8$ kPa (Öncü et al. 2012; Raga and Cossu 2014; Ritzkowski et al. 2016; Townsend et al. 2015).

In summary, to maintain the stability of landfill slope under aeration, a smaller aeration pressure should be adopted for a shorter horizontal distance between the top of the injection screen and the slope surface, *d*. Based on the above numerical modeling, an aeration pressure exceeding 10 kPa is only allowed for $d > 10$ m. The design chart in Fig. 10 (shadow region) can provide some reference values for the air injection pressures at different values of *d*.

Conclusions

This study performs a three-dimensional numerical analysis for landfill slope stability during leachate recirculation and aeration using strength reduction method. The bio-hydro coupled processes of waste are simulated by a previously reported landfill coupled model programmed on the open-source platform OpenFOAM and then incorporated into the analysis. Compared with the previous studies, this study investigates the effects of waste

biodegradation and leachate-gas flow on the stability of a landfill slope and provides some guidelines for leachate recirculation and aeration. The main findings are as follows:

1. The values of factor of safety calculated in this study using strength reduction method and finite volume method agree well with the previous related results, and the acceptable difference is due to the difference in the calculation method and modeling approach.
2. The landfill gas produced by waste biodegradation will significantly affect the values and the distribution of gas pressure in a landfill, and then affect the redistribution of leachate pressure and the slope stability during leachate recirculation. The ignorance of landfill gas flow during leachate recirculation is only reasonable when the organic content of landfilled waste is low and hence waste biodegradation can be ignored. Otherwise, the influence range and the performance of leachate recirculation would be overestimated.
3. Both increasing the leachate injection pressure and the maximum anaerobic biodegradation rate can reduce the *FS* value of the landfill slope maximally by 0.32 and 0.62, respectively, due to the increased pore leachate and gas pressures. If only ignoring the gas flow, the waste biodegradation and the produced leachate have a very slight effect on the landfill slope stability. However, the ignorance of both waste biodegradation and gas flow will significantly overestimate the stability of a landfill slope under leachate recirculation by about 20–50%, especially when the landfilled waste is easily degradable.
4. The *FS* of a landfill slope under aeration shows a significant reduction when the aeration pressure exceeds a critical value and this value is defined as safe aeration pressure. The maximum reduction can reach up to 0.8 (by about 53%). A relationship between the safe aeration pressure and the horizontal distance between the top of the injection screen and the slope surface, *d*, is proposed for preliminary design to avoid landfill slope failure during aeration. A smaller aeration pressure should be adopted when the distance *d* is small, and an aeration pressure exceeding 10 kPa is only allowable for $d > 10$ m.

Abbreviations
MSW: Municipal solid waste; LEM: Limit equilibrium method; SRM: Strength reduction method; FS: Factor of safety; FVM: Finite volume method; FEM: Finite element method; FDM: Finite difference method.

List of symbols
A: The anisotropic coefficient of waste [–]; C_O: The concentration of oxygen in gas phase [ML^{-3}]; D_O: The diffusion coefficient of oxygen in gas [L^{2}T^{-1}]; E_s:

Feng *et al. Geoenvironmental Disasters* (2021) 8:29

Page 15 of 16

The Young's modulus [ML^{-3} T]; f_s: The leachate saturation correction factor [–]; **g**: The gravitational acceleration [LT^{-2}]; **J**$_O$: The diffusive flux of oxygen in gas phase [ML^{-3} T]; $k_{r\alpha}$: The relative permeability of phase α [–]; $k_{A,max}$, $k_{N,max}$: The maximum biodegradation rates under aerobic and anaerobic conditions, respectively [T^{-1}]; k_O: The oxygen half-saturation constant [–]; K_v: The vertical intrinsic permeability of waste [L^2]; **K**$_\alpha$: The tensor field of the permeability of phase α in waste [L^2]; n: The porosity of waste [–]; p_α: The pore pressure of phase α [ML^{-1} T^{-2}]; p_c, p_{c0}: The capillary pressure and the entry capillary pressure of gas, respectively [ML^{-1} T^{-2}]; p_{Og}: The oxygen partial pressure [ML^{-1} T^{-2}]; Q_α: The source term due to biodegradation of phase α [ML^{-1} T^{-3}]; Q_O: The source term of oxygen in gas phase [ML^{-1} T^{-3}]; R_A, R_N: The growth rates of aerobic and anaerobic species, respectively [ML^{-3} T^{-1}]; $R_{A,D}$, $R_{N,D}$: The decay rates of aerobic and anaerobic species, respectively [ML^{-3} T^{-1}]; S: The biodegradable substrate concentration [ML^{-3}]; S_A, S_N: The half-saturation constants of substrates for aerobic and anaerobic species, respectively [ML^{-3}]; S_α: The saturation of phase α [–]; S_{le}, S_m, S_r: The effective, maximum and residual leachate saturations, respectively [–]; X_A, X_N: The concentration of aerobic and anaerobic species, respectively [ML^{-3}]; Y_N, Y_A: The biomass/substrate yield coefficients of anaerobic and aerobic conditions, respectively [–]; Y_O: The mass fraction of oxygen [–]; **u**: The displacement vector [L]; v: The Poisson's ratio [–]; **v**$_\alpha$: The Darcy velocity of phase α [MT^{-1}]; d$\boldsymbol{\varepsilon}^p$: The plastic strain increment [–]; ρ_α: The density of phase α [ML^{-3}]; σ_1', σ_3': The maximum and minimum principal stresses, respectively [ML^{-1} T^{-2}]; $\boldsymbol{\sigma}'$, $\boldsymbol{\sigma}$: The effective stress and total stress, respectively [ML^{-1} T^{-2}]; τ: The tortuosity factor for gas diffusion [–].

Acknowledgements

Authors' contributions
The authors contributed collectively towards the manuscript. The authors are responsible for data collection, project planning and execution. All authors read and approved the final manuscript.

Funding

Availability of data and materials
The data used in this study are available from the corresponding author on reasonable request.

Declaration

Competing interests
The authors declare that they have no competing interests.

Author details
[1]Department of Geotechnical Engineering, Tongji University, Si Ping Road 1239, Shanghai 200092, China. [2]Key Laboratory of Geotechnical and Underground Engineering of the Ministry of Education, Tongji University, Shanghai 200092, China.

References
Beaven R, White J, Braithwaite P (2008) Application of the University of Southampton Landfill Degradation and Transport Model (LDAT) to an aerobic treatment field experiment. Global Waste Management symposium, Colorado

Byun B, Kim I, Kim G, Eun J, Lee J (2019) Stability of bioreactor landfills with leachate injection configuration and landfill material condition. Comput Geotech 108:234–243

Cao BY, Feng SJ, Li AZ (2018) CFD modeling of anaerobic-aerobic hybrid bioreactor landfills. Int J Geomech 18:04018072.1–04018072.10

Clausen J, Damkilde L, Andersen L (2007) An efficient return algorithm for non-associated plasticity with linear yield criteria in principal stress space. Comput Struct 85:1795–1807

Dawson EM, Roth WH, Drescher A (1999) Slope stability analysis by strength reduction. Géotechnique 49:835–840

El-Fadel M, Findikakis AN, Leckie JO (1996) Numerical modelling of generation and transport of gas and heat in landfills I. Model formulation. Waste Manag Res 14:483–504

Feng SJ, Chen ZW, Chen HX, Zheng QT, Liu R (2018) Slope stability of landfills considering leachate recirculation using vertical wells. Eng Geol 241:76–85

Feng SJ, Li AZ, Zheng QT, Cao BY, Chen HX (2019) Numerical model of aerobic bioreactor landfill considering aerobic-anaerobic condition and biostable zone development. Environ Sci Pollut Res 26:15229–15247

Feng SJ, Chen ZW, Zheng QT (2020) Effect of LCRS clogging on leachate recirculation and landfill slope stability. Environ Sci Pollut Res 27:6649–6658

Feng SJ, Chang JY, Zhang XL, Shi H, Wu SJ (2021a) Stability analysis and control measures of a sanitary landfill with high leachate level. J Geotech Geoenviron Eng 147(10): 05021009

Feng SJ, Wu SJ, Zheng QT (2021b) Design method of a modified layered aerobic waste landfill divided by coarse material. Environ Sci Pollut Res 28:2182–2197

Fytanidis DK, Voudrias EA (2014) Numerical simulation of landfill aeration using computational fluid dynamics. Waste Manag 34:804–816

Griffiths DV, Lane PA (1999) Slope stability analysis by finite elements. Géotechnique 49:387–403

Khoei AR, Mohammadnejad T (2011) Numerical modeling of multiphase fluid flow in deforming porous media: a comparison between two- and three-phase models for seismic analysis of earth and rockfill dams. Comput Geotech 38:142–166

Kim S-Y, Tojo Y, Matsuto T (2007) Compartment model of aerobic and anaerobic biodegradation in a municipal solid waste landfill. Waste Manag Res 25:524–537

Koerner RM, Soong TY (2000) Leachate in landfills: the stability issues. Geotext Geomembr 18:293–309

Lavigne F, Wassmer P, Gomez C, Davies TA, Sri Hadmoko D, Iskandarsyah TYWM, Gaillard JC, Fort M, Texier P, Boun Heng M, Pratomo I (2014) The 21 February 2005, catastrophic waste avalanche at Leuwigajah dumpsite, Bandung, Indonesia. Geoenviron Disasters 1:10

Lu SF, Feng SJ (2020) Comprehensive overview of numerical modeling of coupled landfill processes. Waste Manag 118:161–179

Lu SF, Xiong JH, Feng SJ, Chen HX, Bai ZB, Fu WD, Lü F (2019) A finite-volume numerical model for bio-hydro-mechanical behaviors of municipal solid waste in landfills. Comput Geotechn 109:204–219

Lu SF, Feng SJ, Zheng QT, Bai ZB (2020) A multi-phase, multi-component model for coupled processes in anaerobic landfills: theory, implementation and validation. Géotechnique 71:826–842

Ma J, Liu L, Yu X, Fei XC, Zhang X, Zeng G, Bi YZ (2020) Simulation of gas concentration during the process of air injection and Extraction in a Landfill. Environm Prog Sustain Energy 39:e13406

Meima JA, Naranjo NM, Haarstrick A (2008) Sensitivity analysis and literature review of parameters controlling local biodegradation processes in municipal solid waste landfills. Waste Manag 28:904–918

Millington RJ, Quirk JP (1961) Permeability of porous solids. Trans Faraday Soc 5:1200–1207

Mualem Y (1976) A new model for predicting the hydraulic conductivity of unsaturated porous media. Water Resour Res 12:513–522

Omar H, Rohani S (2017) The mathematical model of the conversion of a landfill operation from anaerobic to aerobic. Appl Math Model 50:53–67

Öncü G, Reiser M, Kranert M (2012) Aerobic in situ stabilization of Landfill Konstanz Dorfweiher: leachate quality after 1year of operation. Waste Manage 32:2374–2384

Raga R, Cossu R (2014) Landfill aeration in the framework of a reclamation project in Northern Italy. Waste Manag 34:683–691

Feng *et al. Geoenvironmental Disasters*   (2021) 8:29

Page 16 of 16

Ritzkowski M, Stegmann R (2012) Landfill aeration worldwide: concepts, indications and findings. Waste Manag 32:1411–1419

Ritzkowski M, WalkeR B, Kuchta K, Raga R, Stegmann R (2016) Aeration of the teuftal landfill: field scale concept and lab scale simulation. Waste Manag 55:99–107

Stegmann R (2019) Development of waste management in the last 30 years. In: Zhan L, Chen Y, Bouazza A (eds) Proceedings of the 8th international congress on environmental geotechnics volume 1. Springer Singapore, Singapore, pp 172–185

Stoltz G, Tinet AJ, Staub MJ, Oxarango L, Gourc JP (2012) Moisture retention properties of municipal solid waste in relation to compression. J Geotech Geoenviron Eng 138:535–543

Tang T, Hededal O, Cardiff P (2015) On finite volume method implementation of poro-elasto-plasticity soil model. Int J Numer Anal Methods Geomech 39:1410–1430

Tchobanoglous G, Eliassen R, Theisen H (1993) Integrated solid waste management: engineering principles and management issues. New York (N.Y.): McGraw-Hill International Editions

Townsend TG, Powell J, Jain P, Xu QY, Tolaymat T, Reinhart D (2015) Landfill air addition, sustainable practices for landfill design and operation, pp 313–343

van Genuchten MT (1980) A closed-form equation for predicting the hydraulic conductivity of unsaturated soils. Soil Sci Soc Am J 44:892–898

Weller HG, Tabor G (1998) A tensorial approach to computational continuum mechanics using object-oriented techniques. Comput Phys 12:620–631

Xu QY, Tolaymat T, Townsend TG (2012) Impact of pressurized liquids addition on landfill slope stability. J Geotech Geoenviron Eng 138:472–480

Yuan W, Li J, Li Z, Wang W, Sun X (2020) A strength reduction method based on the Generalized Hoek–Brown (GHB) criterion for rock slope stability analysis. Comput Geotech 117:103240

Publisher's Note